Szymon LIPIŃSKI[1], Jan ZAWILAK[1]

Wroclaw University of Technology (1)

Three-Dimensional Thermal Model of a Line-Start Permanent Magnet Synchronous Motor Using Computational Fluid Dynamics

Abstract. *An analysis of heat transfer in a low power line-start permanent magnet synchronous motor is presented. A three-dimensional numerical model together with its experimental verification are reported. The model takes into account the mixed convection and heat conduction inside the motor. Radiative heat transfer is assumed to be negligible due to relatively low temperature difference between the motor's surface and the environment. The analysis was performed for steady state operation conditions at rated load. To determine the loss density distribution in the motor, electromagnetic calculations were performed. The temperature distribution on the surface of the frame in a steady state calculated numerically was compared with pictures taken with an infrared camera. To verify the thermal images four thermocouples placed on the frame were used. Furthermore, the surface temperature of the rotor was measured using pyrometers.*

Streszczenie. *W pracy opisano analizę wymiany ciepła w silniku synchronicznym małej mocy o rozruchu bezpośrednim i jego otoczeniu. Zaprezentowano trójwymiarowy numeryczny model cieplny obiektu oraz jego weryfikację doświadczalną. Model uwzględnia konwekcję naturalną i wymuszoną oraz przewodzenie ciepła wewnątrz silnika. Oddawanie ciepła przez promieniowanie pominięto, jako nieznaczące ze względu na zbyt niską różnicę temperatur powierzchni i otoczenia. Analizę przeprowadzono w stanie ustalonym podczas pracy silnika ze znamionowym obciążeniem. W celu wyznaczenia rozkładu gęstości strat w silniku wykonano obliczenia na modelu elektromagnetycznym. Rozkład temperatury na powierzchni korpusu w stanie ustalonym obliczony metodą numeryczną i porównano ze zdjęciami wykonanymi kamerą termowizyjną. Do weryfikacji termogramów uzyskanych przy pomocy kamery termowizyjnej wykorzystano cztery termopary umieszczone w korpusie. Ponadto zmierzono temperaturę powierzchni czołowej wirnika wykorzystując pirometry. (**Trójwymiarowy model cieplny silnika synchronicznego z magnesami trwałymi o rozruchu bezpośrednim przy zastosowaniu obliczeniowej mechaniki płynów**)*

Keywords: synchronous motor, permanent magnets, line-start, thermal analysis, computational fluid dynamics
Słowa kluczowe: silnik synchroniczny, magnesy trwałe, rozruch bezpośredni, analiza termiczna, obliczeniowa mechanika płynów

Introduction

During design of an electrical machine it is necessary to perform thermal calculations to predict temperature of its components. Because many of the materials used in the construction of electrical machines change significantly their properties with temperature, the influence of heating on the electromechanical characteristics such as efficiency or the electromagnetic torque should be taken into account. Therefore, thermal analysis allows to improve the overall accuracy of the computations of electromechanical properties [1]. Moreover, excessive operating temperature of the winding leads to their degradation and early failure [2]. Hence, accurate calculation of the temperature distribution in the machine is an important issue. Among the methods available, the latest one employs calculations using Computational Fluid Dynamics [3]. Solving flow equations using Finite Volume Method for the three-dimensional geometry allows to calculate the flow of air forced by the fan. On this basis, it is possible afterwards to determine the distribution of heat transfer coefficient to the entire surface of the motor. The resulting heat transfer coefficient is then used as a boundary condition for the heat conduction equation inside the machine. Losses calculated in the electromagnetic model will provide the necessary information to define the heat sources in the thermal model of the Line-Start Permanent Magnet Synchronous Motor during the steady-state operation.

Electromagnetic model

The losses in the machine were determined by modeling the LSPMSM in Ansys Maxwell v16.2. It has a stator and a mechanical structure based on the induction motor Sh90 L-4. The rotor from the original motor was replaced with one with permanent magnets buried inside the squirrel cage.

The software solves the following equation

$$(1) \quad \nabla \times \frac{1}{\mu} \nabla \times A = J_s - \sigma \nabla V + \nabla \times H_c + \sigma v \times \nabla \times A,$$

where: μ is the magnetic permeability, A is the magnetic vector potential, J_s is the source current density, σ is the electric conductivity, V is the electric potential, H_c is the coercivity of the permanent magnet, v is the velocity of moving parts [4].

The losses were determined for the rated operating conditions: line voltage equal to 400 V and a frequency of 50 Hz and a time constant load equal to 1900 W. As a boundary condition assumed zero normal component of the vector potential on the outer perimeter of the stator. The two-dimensional geometry was divided into 16 378 triangular elements as shown in Fig. 1.
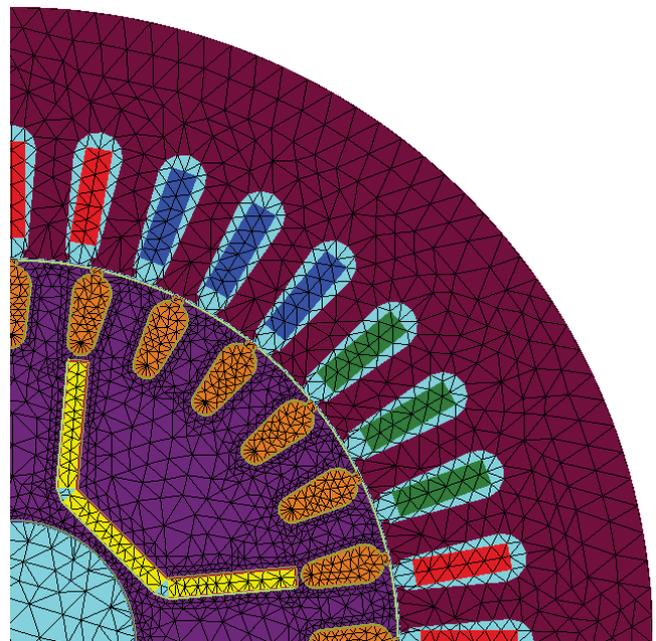

Fig. 1. A quarter of the mesh used in Finite Element Analysis

Computational fluid dynamics model

In order to estimate the distribution of the heat transfer coefficient on the surface of the motor, it is necessary to determine the flow of the air forced by a fan mounted on the shaft. To do this, a three-dimensional geometry of the fan and motor was created incorporating the necessary simplifications. The omission of small details of geometry allows to

keep better mesh quality while maintaining a fixed number of elements. It is a compromise between accuracy and computational effort. The model uses two reference systems. The first, stationary, corresponds to the domain of fluid around the machine. The second domain includes a fluid surrounded by a fan. For each of the domains are created separated meshes, which combined contain total considered volume, wherein the calculations are made.

In the domain connected to the rotating reference frame omitted of the wall thickness of the fan blades and provided the structural mesh comprising approx. 260,000 hexahedral elements. The volume associated with the fixed reference frame was divided using unstructured tetrahedral mesh containing approx. 2.5 million elements (Fig. 2). The unstructured mesh was used due to difficulties with building a block structure for such a complex geometry as the electric motor. The shape of this domain is a cuboid with a "subtracted" volume of the motor and the domain associated with the fan.

On the walls of the fan it is assumed no-slip condition. Furthermore, it is assumed that the surface is adiabatic. On the walls of the motor it is assumed also no-slip condition of the fluid. In addition, it is assumed that the surfaces transferring the heat (e.g. ribbed body, bearing shields) are isothermal. The calculations were performed for air pressure of 1013.25 hPa and a temperature of 20°C. For modeling turbulence used a variation of Shear Stress Transport k-ω model. The result of the calculation is the solution of the following Partial Differential Equations

(2) $$\nabla\left(\rho\boldsymbol{U}\right) = 0,$$

(3) $$\nabla\left(\rho\boldsymbol{U}\otimes\boldsymbol{U}\right) = -\nabla p + \nabla\tau + \boldsymbol{S}_{\mathrm{M}},$$

(4) $$\nabla\left(\rho\boldsymbol{U}h\right) = \nabla\left(\lambda\nabla T\right) + \nabla\left(\boldsymbol{U}\tau\right) + \boldsymbol{S}_{\mathrm{E}},$$

complemented by the equations of turbulence model:

(5a) $$\frac{\partial\left(\rho\boldsymbol{U}_i k\right)}{\partial x_i} = P_k + P_{kb} +$$
$$-\beta^*\rho k\omega + \frac{\partial}{\partial x_i}\left[\left(\mu + \frac{\mu_t}{\sigma_{k3}}\right)\frac{\partial k}{\partial x_i}\right],$$

(5b) $$\frac{\partial\left(\rho\boldsymbol{U}_i\omega\right)}{\partial x_i} = \alpha_3\frac{\omega}{k}P_k + P_{\omega b} - \beta_3\rho\omega^2 +$$
$$+ \frac{\partial}{\partial x_i}\left[\left(\mu + \frac{\mu_t}{\sigma_{\omega 3}}\right)\frac{\partial\omega}{\partial x_i}\right] + \left(1 - F_1\right)\frac{2\rho}{\sigma_{\omega 2}\omega}\frac{\partial k}{\partial x_i}\frac{\partial\omega}{\partial x_i},$$

where: $\boldsymbol{U}$ is the vector of velocity, k is the specific turbulence kinetic energy, ω is the specific rate of dissipation of the turbulence kinetic energy, ρ is the density, μ is the dynamic viscosity, μ is the turbulent viscosity, h is the specific total enthalpy, p is the static pressure, λ is the thermal conductivity, T is the static temperature, τ is the shear stress, S_{E}, S_{M} are the sources of energy and momentum respectively, β^*, α_3, β_3, $\sigma_{\omega 2}$, $\sigma_{\omega 3}$, σ_{k3} are the turbulent model constants, P_k i the production limiter, F_1 is the blending function [5, 6]. On the basis of the numerical solution of the above equations in the given domain, it is possible to calculate the distribution of the heat transfer coefficient for a range of temperatures on the motor's surfaces. These results can be used to calculate temperatures inside the motor, or to optimize the cooling system.
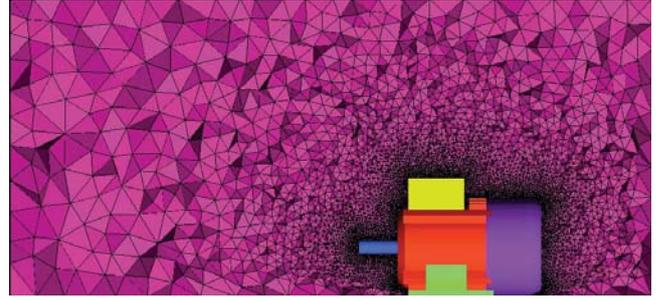

Fig. 2. Cross-section of the domain associated with the fixed reference system

Heat diffusion model

A three-dimensional model of the motor allows to determine the temperature distribution inside the machine. It can be computed using Fourier's equation taking into account the heat conduction and heat sources from the electromagnetic model and the boundary condition obtained from CFD.

Motor's geometry was created based on the electromagnetic model and supplemented with the ribbed frame. It was also necessary to add all the elements omitted in the two-dimensional model, such as the stator coils, end rings of cage and bearings. This allows to use directly boundary conditions obtained from CFD, without the need to calculate the thermal resistance of the frame. Stator windings are replaced by a single lump of constant conductivity taking into account the anisotropy [7]. In the direction across the coils conductivity is much smaller due to wire's insulation and small airgaps. In the coil endings anisotropy is neglected due to the omission of heat transfer in the air filled areas inside the motor. Heat conduction through the air is taken into account only in the air gap. Similarly, anisotropy is considered in the lamination. Both, the active part of the windings and the lamination are assumed to be orthotropic [8]. Thermal resistance at the interface between the individual elements is represented by the equivalent airgap. The multi-body domain is divided into approx. 3.7 million tetragonal elements. The resulting distribution of temperature is given by the solution of the following PDE [9]:

(6) $$\nabla\left(\rho\boldsymbol{U}h\right) = \nabla\left(\lambda\nabla T\right) + \boldsymbol{S}_E,$$
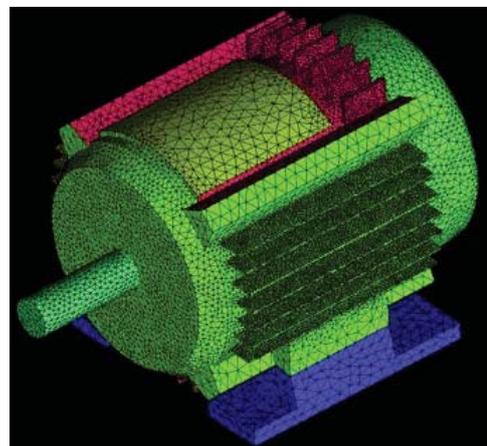

Fig. 3. View of the mesh on the surface of the motor

Results

On the basis of the calculations mentioned before, a three-dimensional temperature distribution inside the motor was obtained. The temperature field in the motor cross sections are shown in Figures 4 and 5. It can be seen that the highest temperature during steady state operation occurs in the rotor. This is caused due to the fact that the heat transfer from the rotor through airgap is hindered, regardless the relatively small losses in rotor volume. Additionally, abrupt changes in temperature resulting from the consideration of contact thermal resistance between the individual lumps are visible. Another important fact is that the bottom part of construction is slightly colder than the upper part, which is caused by reduced heat dissipation due to the terminal box. The insulating divider inside the box impede the heat flux as shown in Figure 6. However, in the windings the most heated zones are in the coil endings.

In the figures 6 and 7 are shown compared the results of calculations and the thermal images obtained after heating the engine to the steady state. Basing on this comparison we can say that the obtained numerically temperature field is the same nature as observed in the real object.
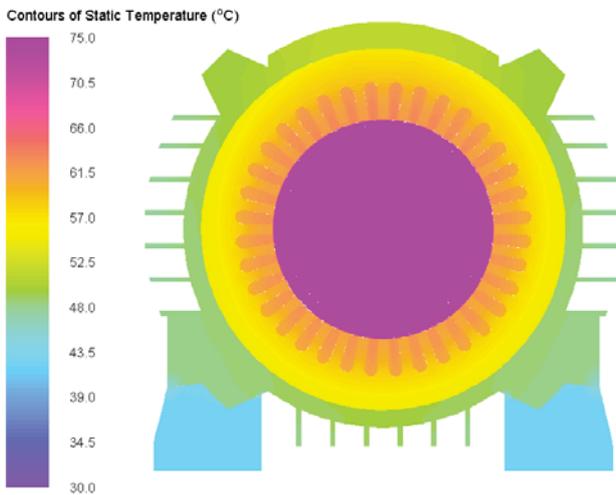

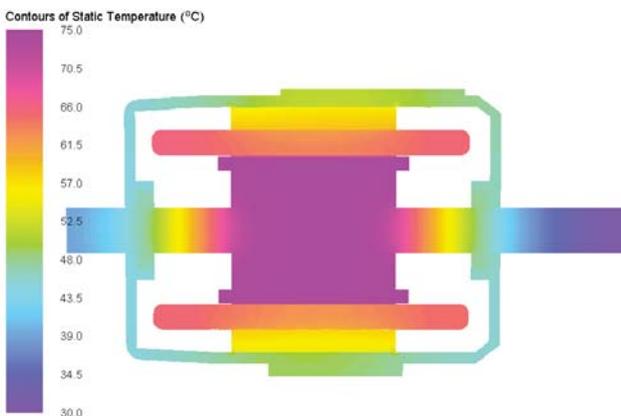Fig. 4. The temperature distribution in the cross section of the machine

Fig. 5. The temperature distribution in the axial section of the machine

Regardless of the use of the infrared camera, thermocouples were used and are visible on the thermal images. They were utilized to measure temperature in particular points on the frame. Moreover, two infrared thermometers mounted on the bearing shield were used to measure the temperature of the rotor. The temperature of the coils
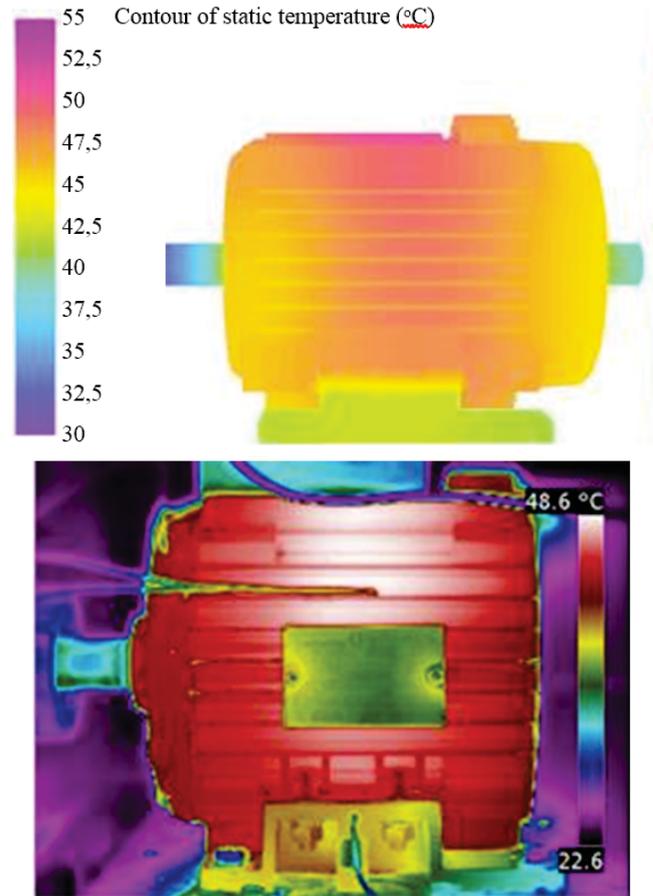

Fig. 6. Comparison of the temperature distribution on the side surface of the motor

was determined by measuring a change in resistance of the engine running and compared with the average temperature obtained by numerical volume weighted average of the entire volume of the windings. Comparison of the results of calculations of the measured values are shown in Table 1.

Table 1. Validation of the thermal model

Spot of measurement	Result of measurement ^oC	Result from thermal image ^oC	Result of calculations ^oC
End of the rib	41.4	45.2	45.6
Middle of the rib	42.5	46.0	47.8
Feet	35.2	37.1	42.3
Shield	43.1	46.1	46.5
Stator winding	64.1	–	64.0
Rotor	72.2	–	74.2

Conclusions

Based on the comparison of the results from the calculations and the measurements on the physical model of the LSPMSM it can be concluded that the presented method can be used to determine the temperature inside the motor. The accuracy of the calculation depends mainly on the precision of determined materials coefficients and thermal contact resistances.

The presented method can be used to calculate the thermal state of electric machinery at the stage of design, as it only requires a defined geometry and material data, together with data resulting from the manufacturing technology. Because model's geometry can be parametric, this method may be used to optimize the cooling system.
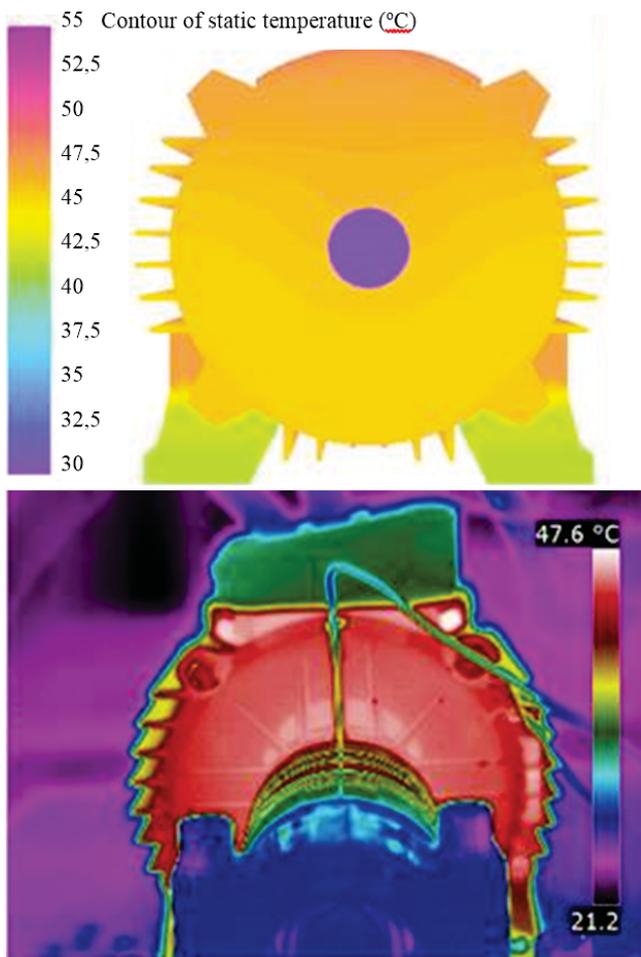
Fig. 7. Comparison of the temperature distribution on the frontal surface of the motor

The authors will continue work on improving the method of thermal calculations to reduce the differences between the calculations, measurements and actual values of temperatures in physical models of LSMPSM.

Acknowledgments

Authors: *M. Sc. Szymon Lipiński, Ph. D. Jan Zawilak, Faculty of Electrical Engineering, Wroclaw University of Technology, ul. Wyspiańskiego 27, 50-370 Wrocław, Poland, email: szymon.lipinski@pwr.edu.pl, jan.zawilak@pwr.edu.pl*

REFERENCES
[1] Lefik M.: Design of permanent magnet synchronous motors including thermal aspects, COMPEL: The International Journal for Computation and Mathematics in Electrical and Electronic Engineering, 34, pp. 561–572, 2015.
[2] Faharani M., Gockenbach E., Borsi H., Shäfer K., Kaufhold M.: Behavior of Machine Insulation Systems Subjected to Accelerated Thermal Aging Test, IEEE Transactions on Dielectrics and Electrical Insulation, 17(5), pp. 1364–1372, 2010.
[3] Boglietti A., Cavagnino A., Staton D., Shanel M., Mueller M., Mejuto C.: Evolution and Modern Approaches for Thermal Analysis of Electrical Machines, IEEE Transactions on Industrial Electronics, 56(3), pp. 871–882, 2009.
[4] ANSYS Maxwell 16.2: Maxwell 2D Technical Notes – Transient Simulation, Maxwell Online Help.
[5] ANSYS CFX 16.2: CFX Modelling Guide & Theory Guide, ANSYS Help Viewer.
[6] Menter F. R., Kuntz M., Langtry R.: Ten years of industrial experience with the SST turbulence model, Turbulence, Heat and Mass Transfer 4, Begell House Inc., 2003.
[7] Idoughi L., Mininger X., Bouillault F., Bernard L., Hoang E.: Thermal Model with Winding Homogenization and FIT Discretization for Stator Slot, IEEE Transactions on Magnetics, 47(12), pp. 4822-4826, 2011.
[8] Furmański P., Gogół W. Podstawy przewodzenia ciepła w ośrodkach anizotropowych, Biuletyn informacyjny Instytutu Techniki Cieplnej Politechniki Warszawskiej, 46, 1977
[9] ANSYS Fluent 16.2: Fluent Theory Guide, ANSYS Help Viewer